Nonlinear Dynamic Response of Frame-Type Structures with Hysteretic Damping at the Joints

G. Shi*
Dalian University of Technology, Dalian, People's Republic of China
and
S. N. Atluri†
Georgia Institute of Technology, Atlanta, Georgia 30332

The dynamic response of frame-type structures with hysteretic damping at the structural joints, resulting from slipping and nonlinear flexible connections, is investigated in this paper. The slipping at a structural joint is represented by the modified Coulomb joint model. The behavior of a nonlinear flexible connection is modeled by the Ramberg-Osgood function. A simple computational model for the dynamic analysis of frames with the hysteretic damping is presented here. Several numerical examples are included, to illustrate the usefulness of the approach in analyzing large space structures.

Nomenclature

A	= transformation matrix for $Q = A\sigma$
a_i, b_i	= parameters used in Eq. (12)
C, M	= viscous damping matrix and mass matrix of a system
Δd, ΔD	= element displacement vectors in the global and local coordinates
EA, GJ, EI_2, EI_3	= tensile, torsional, and flexural rigidity of an element
f, F, F_e	= restoring force, increments of restoring forces of system and elements
F_g	= slipping force in Coulomb joint model
K, K_e	= system and element tangent stiffness matrices
Δh, Δk_i	= increments of axial strains and curvatures of element
l, ΔH	= element length and its incremental change
Δn, Δm_1, $\Delta^\alpha m_i$	= increments of element nodal force and moments
ΔN, ΔM_i	= increments of element "stress" fields
ΔP, P^t, R^t	= increments of loads, and total loads and internal forces up to time t
Q	= element nodal force vector
R	= transformation matrix from element local to global coordinates
S, S^0, S^t	= rigidity, initial rigidity, and instantaneous rigidity of a spring
T, T_i	= element stiffness matrix and its submatrix in element local coordinates
U, $\dot{U}$, $\ddot{U}$	= displacement velocity and acceleration vectors of a system
θ_i^*, ${}^\alpha\theta_i^*$	= element rotation field and nodal rotations measured in element local coordinates
$\Delta\nu$, $\Delta\mu_i$	= variations of ΔN and ΔM_i
$\Delta\sigma$	= increments of element "stress" variables
ϕ, $\Delta^\alpha\phi_i$	= relative deformations at a joint and at element ends

Received Nov. 7, 1990; revision received May 16, 1991; accepted for publication June 13, 1991.

*Research Associate, Research Institute of Engineering Mechanics.

†Regents' Professor and Director, Computational Mechanics Center.

I. Introduction

It is well known that joints or connections are the unavoidable components of a structure. In practice, all types of joints of frame structures are semirigid or flexible.[1] In certain types of joints, the flexible connections behave nonlinearly because of the local distortion and yielding, etc., at the connections. And in other types of joints, slipping between different components at a joint may occur.[2] Under dynamic loading, the nonlinearity of flexible connections and the slipping at structural joints will result in a hysteresis loop in the load vs relative displacement curves. The area enclosed by the loop corresponds to the energy dissipation in a cycle of oscillation. Therefore, the slipping and nonlinear flexible connections lead to hysteretic damping. On Earth, damping primarily arises from aerodynamic effects; consequently the hysteretic damping at joints may not be very important. However, such hysteretic damping is one of the principal sources of energy dissipation in large flexible space structures, and plays a major role for such structures since even a small amount of damping can provide stability to these structures.

Although the study of the hysteresis for a single degree of freedom system has received considerable attention (see, for example, Refs. 2–5 among others), up to now only a few papers have considered the influence of slipping at joints, and nonlinear flexible connections, on the dynamic behavior of multi-degree-of-freedom structures. A common way used in the analysis of slipping for a system with a single degree of freedom is the equivalent linearization[2,5] or the use of the loss coefficient of energy dissipation.[6] The linearization involves the knowledge of frequency of the slipping at the joint, and the concept of a loss coefficient involves the peak potential energy. For a complex or nonlinear structure, it is impossible to know the frequency of slipping at each joint or the peak potential under an arbitrary disturbance. Thus, such linearization or peak potential approaches are not feasible for the hysteretic analysis of complex and nonlinear systems.

With the success of the space shuttle, the dream of building space stations and other structures in outer space becomes closer to reality. Consequently, the dynamics and control of large flexible space structures are topics of current interest.[7] As mentioned earlier, the hysteretic damping at the structural joints is very important for such structures. The purpose of this paper is to study the hysteretic damping resulting from slipping and flexible connections at the joints of structures. In general, the restoring force in a hysteresis system is rate dependent. For example, the friction force at a joint will be a function of the magnitude of the velocity of the relative displacement. However, it is feasible to approximate the friction coefficient as a constant within a certain region of velocity. Since the natural frequencies of these large flexible structures are quite small, the restoring forces for such structures can be approximated to be rate independent.

There are many types of models proposed to represent the behavior of hysteretic systems. Capecchi and Vestroni[5] showed that the bilinear and the Ramberg-Osgood models[8,9] give stable and single valued response curves, while other models may exhibit multivalued responses in a certain frequency range. In this paper, the slipping at a joint is modeled by the modified Coulomb joint model which is bilinear, and the hysteresis loop is traced directly rather than by linearization. The behavior of a nonlinear flexible connection is represented by the Ramberg-Osgood model.[9,10]

In order to apply the modified Coulomb joint model and the Ramberg-Osgood model to the dynamic analysis of large-scale frame-type structures, a simple computational model accounting for hysteretic damping in structural joints is proposed here. This computational model is based on the assumption that a structural member of frame structures can undergo large rigid rotations and large translations, but small relative rotations and small stretching. Under such an assumption together with use of linearization in each time step, the element tangent stiffness matrix can be decomposed into two parts: 1) the common linear stiffness matrix, and 2) the initial stress stiffness matrix. The primary objective of this study is to present the formulation of the linear stiffness matrix in the presence of relative deformations in the joints of frame structures, since it is this linear stiffness matrix that is affected directly by the relative deformations at structural joints. The proposed computational model can be easily incorporated in the conventional beam element models, and can be used in the dynamic analysis of large flexible space structures.

II. Equation of Motion

For time $t + \Delta t$, the equation of motion of a discretized system with nonlinear flexible connections and slipping at joints can be written in an incremental form as

$$M\Delta\ddot{U} + C\Delta\dot{U} + F(U, \Delta U, Q) = \Delta P + P^t - R^t \quad (1)$$

where M, C, and F are, respectively, the mass matrix, viscous damping coefficient matrix, and the incremental restoring force vector of the system; $\Delta\ddot{U}$, $\Delta\dot{U}$, and ΔP are, respectively, the increments of acceleration $\ddot{U}$, velocity $\dot{U}$, displacement U, and external force vector P from time $t + \Delta t$; Q is the internal force vector due to the previous deformation of the system; P^t and R^t are the external force vector and the generalized internal force vector corresponding to the previous time step.

In Eq. (1), M and C can be established in the usual ways. However, F is a function of previous displacement U, initial internal force Q, and the increment of displacement ΔU. Once F is obtained, Eq. (1) can be solved by any time integration scheme. Therefore, evaluating F is the crucial step in the analysis of hysteresis systems. As pointed out in the "Introduction," the objective here is not to consider general hysteresis systems, but to study the influence of hysteretic damping resulting from slipping at joints, and nonlinear flexible connections, on the dynamic responses of framed structures.

III. Restoring Forces for Slipping at Joints

The dry friction, or the so-called Coulomb friction, exists in the components of some types of joints such as bolted connections, pinned junctions, and other proposed joints for outer space structures.[6] Because of the friction, a joint behaves rigidly when the forces at the joint are small. But when the forces reach certain values, the slipping (i.e., relative displacement) between the components of the joint will occur. Therefore, the friction forces play a very important role for the behavior of such types of joints.

Such a joint can be modeled by a simple nonlinear Coulomb joint model[2] which consists of a parallelly connected spring and a Coulomb damper. The rigidity of the spring is denoted by S, and the slipping force is represented by F_g. These two parameters can be determined by experiments.[2] After the slipping occurs, the restoring force f at the joint is given in the Coulomb joint model, as

$$f = S \cdot \phi + \mathrm{sgn}(\dot{\phi})F_g \quad (2)$$

in which ϕ is the relative displacement at the joint; $S \cdot \phi$ is the elastic restoring force contributed by the spring; $\mathrm{sgn}(\dot{\phi})F_g$ gives the Coulomb friction force which approximates the falling characteristics of the dry friction between the components of the joint. The model is illustrated in Fig. 1a.

The Coulomb joint model is bilinear in which the initial rigidity is infinite, and the rigidity of the spring is S. The falling characteristic $[\mathrm{sgn}(\dot{\phi})F_g]$ results in a discontinuity in the hysteresis loop at the points where ϕ changes its sign. It is evident that the discontinuity will cause some numerical difficulty in the analysis. Gaul[2] overcame the difficulty by an equivalent linearization which is based on the harmonic balance for one-dimensional beams. As pointed out earlier, such equivalent linearization is not valid for complex structures. The remedy proposed here is to replace the infinite rigidity by a finite but large enough quantity S^0 (as shown in Fig. 1b). This model is called the modified Coulomb joint model here. The modified Coulomb joint model is a common bilinear model. The hysteresis loop is controlled by the slipping force F_g, an unloading criterion $\mathrm{sgn}(\dot{\phi})$, and a reloading criterion. The modified Coulomb joint model has to keep the same reloading criterion as that in the Coulomb joint model, that is

$$|F_u - F_r| = 2F_g(1 + S/S_0) \quad (3)$$

where F_u and F_r denote the restoring forces at the instants of unloading and reloading, respectively. Since $S/S_0 < 1$, it is feasible to take $|F_u - F_r| = 2F_g$ as the reloading criterion.

After the restoring force reaches the slipping force F_g, the restoring force in the modified Coulomb joint model can be written in an incremental form as

$$\Delta f = S^t \cdot \Delta\phi; \qquad f = F_g + \Sigma\Delta f \quad (4)$$

in which S^t takes on values, respectively, of S and S^0 as indicated in Fig. 1b. On the other hand, the increment $\Delta\phi$ of the relative displacement can be expressed by

$$\Delta\phi = \Delta f / S^t \quad (5)$$

Here the relative displacement ϕ is a generalized one. It can be a relative translation or a relative rotation at a joint.

Equations (3–5) are the relations of the restoring force and relative displacement at a joint. For a frame structure, the force-deformation relation needs to be established for a structural member. A structural member, with a Coulomb joint

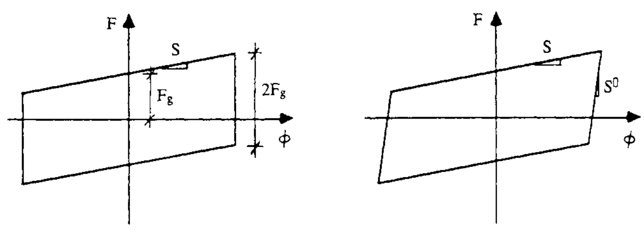

a) Coulomb Joint Model b) Modified Coulomb Joint model

Fig. 1 The hysteresis loop resulting from the friction at a joint.

at its ends, can be modeled by a beam-column element with bilinear springs at the ends. Taking a relative rotation at a joint as an example, a typical element is illustrated in Fig. 2, where $\boldsymbol{x}'$ is the element local coordinate before deformations, and $\hat{\boldsymbol{x}}$ is the current local coordinate of the element after deformations. For an element with constant axial force and torsional moment, and linear bending moments (see "Appendix"), the increments of element force and deformation vectors $\Delta\boldsymbol{D}$, in the element corotational local coordinates, may be defined as

$$\Delta\sigma = \{\Delta n, \Delta m_1, \Delta^1 m_2, \Delta^2 m_2, \Delta^1 m_3, \Delta^2 m_3\}^T \tag{6}$$

$$\Delta\boldsymbol{D} = \{\Delta H, (\Delta^1\theta_1^* - \Delta^2\theta_1^*), -\Delta^1\theta_2^*, \Delta^2\theta_2^*, -\Delta^1\theta_3^*, \Delta^2\theta_3^*\}^T \tag{7}$$

where n is the axial force, ${}^\alpha m_i (i = 2, 3; \alpha = 1, 2)$ is the moment about the element principal axis $\hat{x}_i$ at end α; H and ${}^\alpha\theta_i^*$ are their work-conjugate deformations. In the case of the presence of rotational springs at the element ends shown in Fig. 2, the increments of the nodal rotations $\Delta^\alpha\theta_i^*$ $(i = 2, 3; \alpha = 1, 2)$ consist of two parts, that is

$$\Delta^\alpha\theta_i^* = \Delta^\alpha\theta_i^{**} + \Delta^\alpha\phi_i, \qquad i = 2, 3; \alpha = 1, 2 \tag{8}$$

where $\Delta^\alpha\theta_i^{**}$ is the part resulting from the elastic beam, and $\Delta^\alpha\phi_i$ is the contribution of the rotational springs. If one lets ${}^\alpha S_i^t$ be the instantaneous rigidities of the rotational springs about the $\hat{x}_i$ axis at node α, then the incremental rotations of the rotational springs take the form

$$\Delta^\alpha\phi_i = (-1)^\alpha \frac{\Delta^\alpha m_i}{{}^\alpha S_i^t}, \qquad i = 2, 3; \alpha = 1, 2 \tag{9}$$

By using the weak form of the compatibility conditions of a beam element, one can obtain (see "Appendix" for the derivation) that $\Delta\sigma$ and $\Delta\boldsymbol{D}$ have the following relationship for a linear elastic beam element with springs at its ends:

$$\Delta\sigma = \boldsymbol{T}\Delta\boldsymbol{D} \tag{10}$$

in which $\boldsymbol{T}$ is the element stiffness matrix in the *element corotational local coordinates* and is of the form:

$$\boldsymbol{T} = \begin{bmatrix} EA/l & & & \boldsymbol{O} \\ & GJ/l & & \\ \boldsymbol{O} & & T_2 & \\ & & & \boldsymbol{T}_3 \end{bmatrix} \tag{11}$$

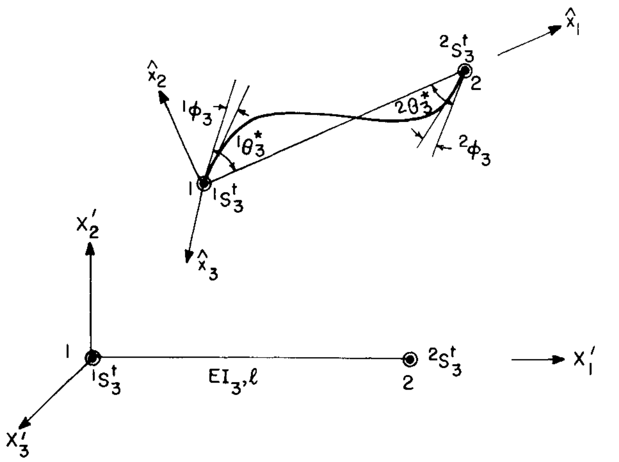

Fig. 2 A typical beam-column element with rotational springs at the ends in $\hat{x}_1 - \hat{x}_2$ plane.

with

$$\boldsymbol{T}_i = \frac{6EI_i}{l(2 + a_i)(2 + b_i) - 1} \begin{bmatrix} (2 + b_i) & -1 \\ -1 & (2 + a_i) \end{bmatrix}$$

$$(i = 2, 3) \tag{12}$$

$$a_i = \frac{6EI_i}{{}^1S_i^t l}, \qquad b_i = \frac{6EI_i}{{}^2S_i^t l}$$

In the above equations EA is the tensile stiffness of the element, GJ is the torsional rigidity, EI_i $(i = 2, 3)$ is the flexural rigidity about axis $\hat{x}_i$, and l is the element length; a_i and b_i are the modifying terms contributed by the rotational springs at the element ends. It is evident that a_i and b_i approach to zero as ${}^1S_i^t$ and ${}^2S_i^t$ approach infinity, i.e., $\boldsymbol{T}$ goes back to the element stiffness matrix in the local coordinates for the case of rigidly connected frames.

The element nodal force vector defined in the element local coordinates $\boldsymbol{Q}$ is of the form

$$\boldsymbol{Q}^T = [n, Q_2, Q_3, m_1, {}^1m_2, {}^1m_3, n, Q_2, Q_3, m_1, {}^2m_2, {}^2m_3] \tag{13}$$

in which $Q_2 = ({}^1m_3 - {}^2m_3)/l$ and $Q_3 = ({}^2m_2 - {}^1m_2)/l$ are the nodal transverse shear forces. The incremental nodal displacement vector of an element measured in the global reference system $\Delta\boldsymbol{d}$ is defined as

$$\Delta\boldsymbol{d} = \{\Delta^1u_1, \Delta^1u_2, \Delta^1u_3, \Delta^1\theta_1, \Delta^1\theta_2, \Delta^1\theta_3, \Delta^2u_1, \Delta^2u_2, \Delta^2u_3, \Delta^2\theta_1, \Delta^2\theta_2, \Delta^2\theta_3\}^T \tag{14}$$

By denoting the transformation matrix from the element local coordinates to the global reference system by $\boldsymbol{R}$(a 12 × 12 matrix), and denoting the transformation from σ to $\boldsymbol{Q}$ by A (a 12 × 6 matrix), i.e., $\boldsymbol{Q} = \boldsymbol{A}\sigma$, then the incremental nodal displacement vectors $\Delta\boldsymbol{D}$ and $\Delta\boldsymbol{d}$ measured in the element local coordinates and the global reference system, respectively, have the following relationship:

$$\Delta\boldsymbol{D} = (\boldsymbol{R}\cdot\boldsymbol{A})^T\Delta d \tag{15}$$

Consequently, for a beam-column element undergoing large deformations but small strains (geometrical nonlinearity), the incremental restoring force vector $\boldsymbol{F}_e$ of an element measured in the global reference system takes the form:

$$\begin{aligned}\boldsymbol{F}_e &= (\boldsymbol{R}\cdot\boldsymbol{A})\boldsymbol{T}(\boldsymbol{R}\cdot\boldsymbol{A})^T\Delta\boldsymbol{d} + \boldsymbol{K}_s(\boldsymbol{U}, \boldsymbol{Q})\Delta\boldsymbol{d} \\ &= [\boldsymbol{K}_l + \boldsymbol{K}_s(\boldsymbol{U}, \boldsymbol{Q})]\Delta\boldsymbol{d} = \boldsymbol{K}_e\Delta\boldsymbol{d}\end{aligned} \tag{16}$$

where $\boldsymbol{K}_l$ is the linear stiffness matrix of an element, $\boldsymbol{K}_s$ is the so-called initial stress stiffness matrix due to large displacements, and $\boldsymbol{K}_e$ is the element tangent stiffness matrix. A formulation for $\boldsymbol{K}_s$ based on the assumed stress fields and the weak form of governing equations was given by Shi and Atluri.[11] These details are not repeated here. It should be noticed that $\boldsymbol{K}_l$ is composed of S_i and S_i^0 $(i = 2, 3)$ according to loading and unloading in the hysteresis loop caused by slipping; and the reloading criterion given by Eq. (3) has to be satisfied at all joints where the slipping is present.

Having obtained the restoring force vector $\boldsymbol{K}_e\Delta\boldsymbol{d}$ for each element, the equation of motion of a system can be written as

$$\boldsymbol{M}\Delta\ddot{\boldsymbol{U}} + \boldsymbol{C}\Delta\dot{\boldsymbol{U}} + \sum_{\text{elem}} (\boldsymbol{K}_e\Delta\boldsymbol{d}) = \Delta\boldsymbol{P} + \boldsymbol{P}^t - \boldsymbol{R}^t \tag{17}$$

together with given initial conditions. Now Eq. (1) becomes a common initial value problem as shown by Eq. 17. It can be seen from Eq. (16) that the initial stress stiffness matrix $\boldsymbol{K}_s$ is also affected by the falling characteristic of dry friction, since $\boldsymbol{K}_s$ also depends on the internal force $\boldsymbol{Q}$, and $\boldsymbol{Q}$ changes abruptly when any slipping at the element ends changes its sign.

IV. Restoring Forces for Nonlinear Flexible Connections

The standardized moment-rotation relation at a flexible beam-column connection can be described by the Ramberg-Osgood model[9] as

$$\frac{\phi}{\phi_0} = \frac{KM}{(KM)_0}\left\{1 + \left[\frac{KM}{(KM)_0}\right]^{n-1}\right\} \tag{18}$$

in which ϕ and M are respectively the relative rotation and its corresponding bending moment at the connection; ϕ_0, $(KM)_0$ and $n[n > 1$, it should be noted that n here is a parameter, not the axial force in Eq. (13)] are parameters that define the shape of moment-rotation curves. For a given type of connection, these three parameters can be determined by the size parameters of the connection.[9] As illustrated in Fig. 3, when the hysteresis loop is undergoing loading, the instantaneous rotational rigidity S^t of the connection described by Eq. (18) is given by[10]

$$S^t = \frac{\mathrm{d}M}{\mathrm{d}\phi} = \frac{S^0}{1 + n\left[\dfrac{K|M|}{(KM)_0}\right]^{n-1}} \tag{19}$$

where S^0 is the initial rigidity, and is of the form

$$S^0 = \left.\frac{\mathrm{d}M}{\mathrm{d}\phi}\right|^{m=0} = \frac{KM_0}{\phi_0 K} \tag{20}$$

Where the hysteresis loop is undergoing unloading, the instantaneous rigidity takes the value of the initial rigidity, i.e., $S^t = S^0$. Therefore, in this case the hysteresis loop is determined by the Ramberg-Osgood function, the unloading or reloading criterion, and the initial rigidity S^0. Let M be the total bending moment at the connection and ΔM be its increment, then the unloading criterion is

$$M \cdot \Delta M < 0 \tag{21}$$

and the reloading is determined by $M \cdot \Delta M > 0$.

The behavior of a nonlinear flexible connection of frame-type structures can be represented by a nonlinear rotational spring in which the rigidity of the spring is equal to S^t. Consequently, the structural member of a flexibly connected frame can be modeled by a beam-column element with rotational springs at the element ends. Therefore, the element local stiffness matrix $\boldsymbol{T}$ defined in Eq. (11) is also valid for an element with nonlinear flexible connections at the ends. However, it should be noticed that the rigidity of a spring in this case varies continuously rather than bilinearly as in the case of slipping at a joint. Furthermore, the unloading and reloading criterions are checked for each bending moment component at every connection individually. Similar to Eq. (16), the incremental restoring force vector for an element with nonlinear flexible connections can be written in a general form as

$$\boldsymbol{F}_e = \boldsymbol{K}_e(\boldsymbol{U}, \boldsymbol{Q}, \boldsymbol{S}^t)\Delta \boldsymbol{d} \tag{22}$$

in which $\boldsymbol{S}^t$ is the instantaneous rigidity vector of rotational springs at the element ends.

It is interesting to compare the behavior of a hysteresis loop resulting from slipping at a joint with that resulting from a nonlinear flexible connection. When the nonlinear flexible connection is approximated by a bilinear model, it seems that they have a similar hysteresis loop. But in fact the hysteresis loop in each case has a different characteristic. For a damped oscillation at a joint, the bilinear hysteresis loop for a nonlinear flexible connection will shrink as the magnitude of the relative displacement decreases in each cycle; and when the bending moment at the connection is less than the "slipping moment," the loop will vanish, i.e., the motion at the connection will only be in the linear region. However, the hysteresis loop resulting from the slipping, on one hand, contracts as the relative displacement decreases, but on the other hand, has to satisfy the falling characteristics of the friction force given in Eq. (3) during the whole vibration, and the hysteresis loop exists until the vibration is totally damped out.

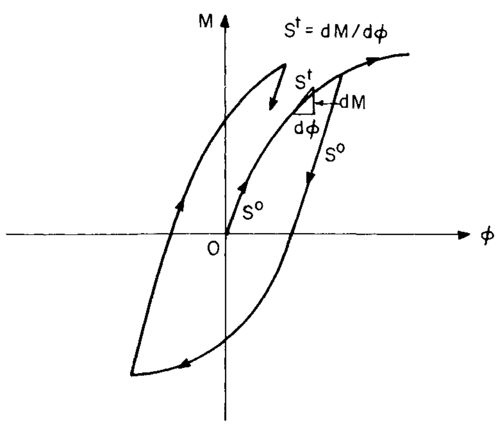

Fig. 3 The hysteresis loop resulting from the nonlinearity of a flexible connection.

V. Numerical Examples

The application of the proposed model is demonstrated by the following three examples. Two structures are considered here: a simple space frame and a three-story plane frame. Since not much information about dynamic response of frames with hysteretic damping at joints is available for comparison, the studies reported herein are much less ambitious.

A. Space Frame with Joint Slipping

Beskos and Narayanan[12] studied the dynamic response of the rigidly jointed frame shown in Fig. 4. Here the frame is assumed to be rigidly jointed to the ground, but to be connected in such a way that in the top level relative rotation can occur at any beam-column connection, with $F_g = 7 \times 10^5$ and $S = 0.1\,EI/l$. The dynamic responses with and without slipping at the joints and to rigid joints are shown in Fig. 4. It can be seen that the slipping at the joints influences the dynamic response quite significantly.

B. Three-Story Frame with Nonlinear Flexible Connections

The three-story single bay frame shown in Fig. 5 is taken from Arbabi's paper,[13] but Arbabi only gave the lateral displacements of the frame with linear flexible connections. A concentrated mass, $M = 100$ lb $-$ s^2/in. at each node and the midspan of the beams is used. The behavior of the connection and the history of the load are depicted in Fig. 5. The responses corresponding to linear flexible connections and nonlinear flexible connections are illustrated in Fig. 5 which shows that the hysteretic damping resulting from the nonlinearity of connections affects both the frequency and amplitude of the response considerably.

C. Three-Story Frame with Joint Slipping

This example concerns the plane frame shown in Fig. 5 with slipping at the joints. A bilinear model with $f_g = 2.5 \times 10^6$,

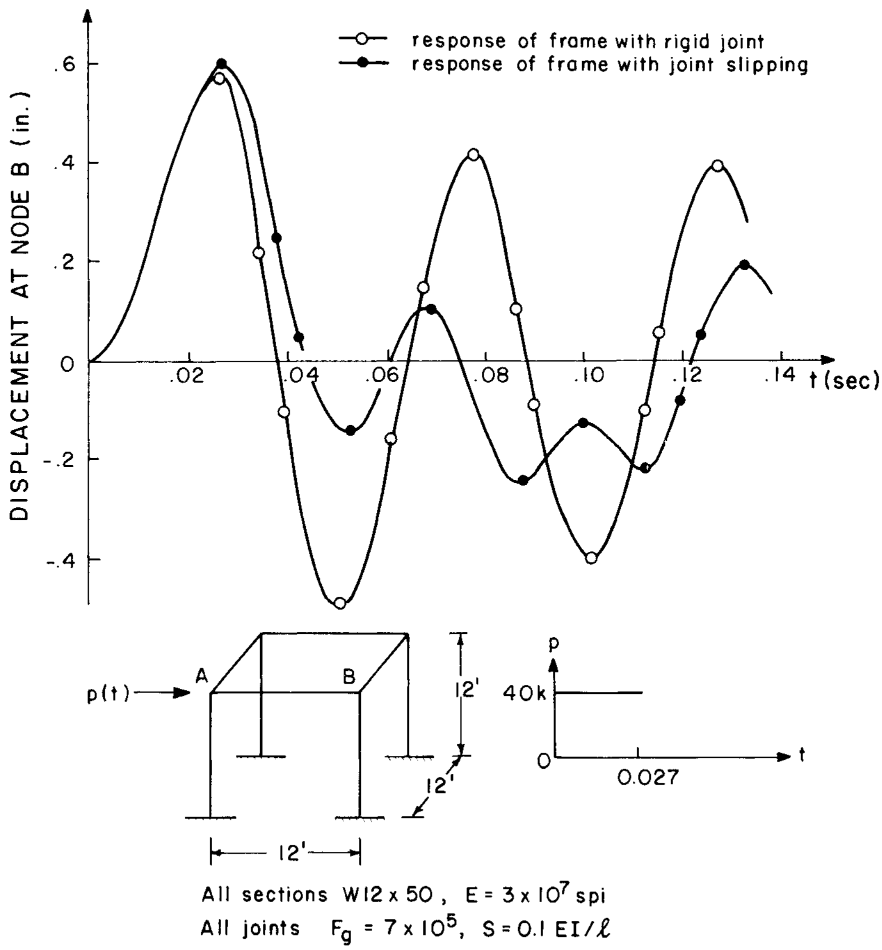

Fig. 4 The geometry, load history, and dynamic response of space frame.

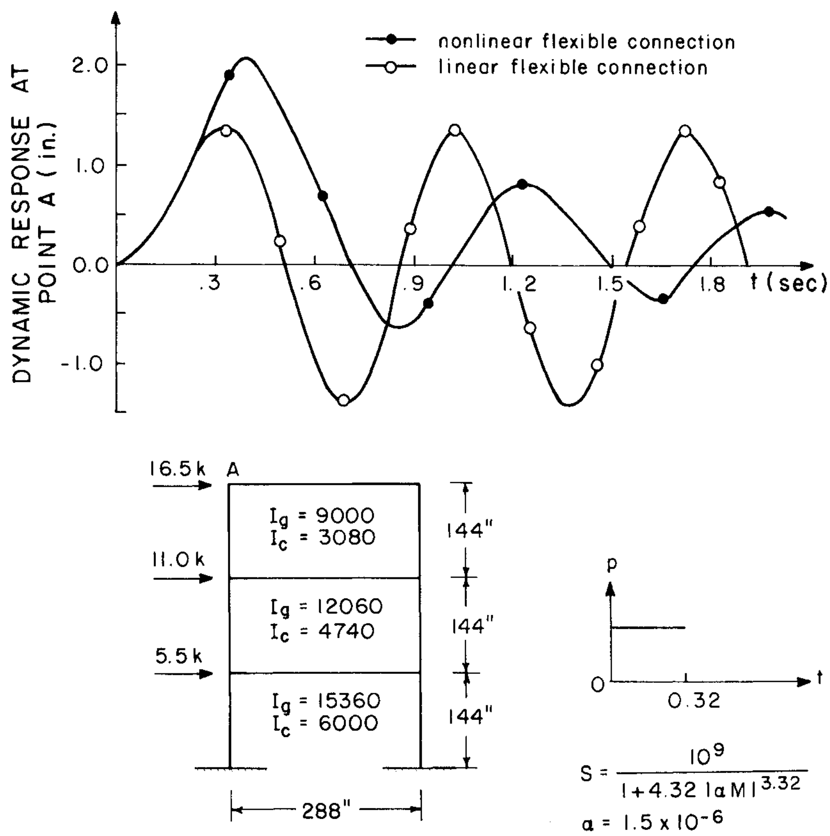

Fig. 5 The dynamic responses of three-story frame with linear and nonlinear flexible connections.

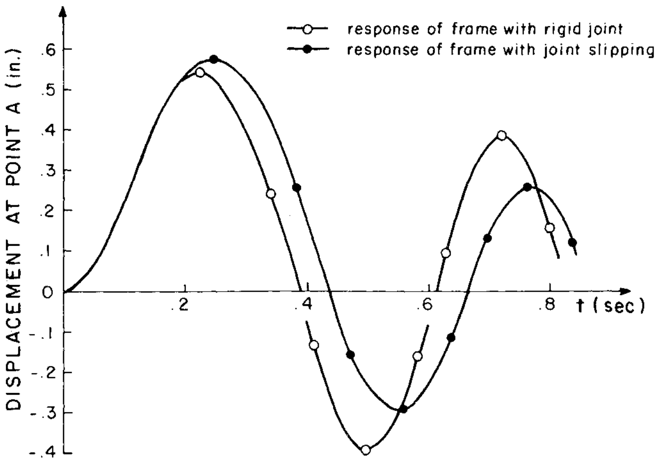

Fig. 6 Dynamic responses of three-story frame with rigid joint and slipping at joints.

$S = 0.1\ EI/l$, and $S^0 = 10^5 \times S$ is adopted. The dynamic responses of both the rigidly jointed frame and the frame with slipping at the joints are plotted in Fig. 6. Once again the hysteretic damping increases the frequency of the vibration and decreases the amplitude of the response.

VI. Closure

The hysteretic damping resulting from the slipping and nonlinear flexible connections at the joints of frame-type structures are studied in this work. The modified Coulomb joint model proposed here is a simple and effective model to represent the slipping at the joints of frames. The Ramberg-Osgood model with the instantaneous rigidity presented here is an efficient means to describe the behavior of nonlinear flexible connections of frames. The presented computational model to account for the hysteretic damping at the structural joints, namely, an elastic beam element with nonlinear springs at the ends, is very simple and accurate for the analysis of frame-type structures. This computational model will be very useful in the dynamic analysis of large flexible space structures.

Appendix: Derivation of Eq. (10)

The detailed derivation of Eq. (10) can be found in Ref. 10. For self-completeness, a brief derivation of this equation is given here.

The derivation is based on the incremental scheme and the assumed stress fields. It is assumed that a beam-column element can undergo large rigid translations and rotations, but small strains. From time t to $t + \Delta t$, an element will have axial displacement Δu_1^* and rotations $\Delta\theta_i^*(i = 1, 2, 3)$ about the element local coordinates measured in the corotational local coordinates of the element. Under the assumption of small strains the element incremental axial strain Δh and curvatures $\Delta\kappa_i$, $(i = 1, 2, 3)$ are of the form

$$\begin{aligned} \Delta h &= \Delta u_{1,1}^* \\ \Delta\kappa_1 &= \Delta\theta_{1,1}^* \\ \Delta\kappa_2 &= -\Delta\theta_{2,1}^* \\ \Delta\kappa_3 &= \Delta\theta_{3,1}^* \end{aligned} \tag{A1}$$

If one lets ΔN and $\Delta M_i(i = 1, 2, 3)$ be the increments of the Cauchy stress resultant and stress couples in the corotational element local coordinates, then a suitable trial stress field can be chosen as

$$\begin{aligned} \Delta N &= \Delta n \\ \Delta M_1 &= \Delta m_1 \\ \Delta M_2 &= (1 - \hat{x}_1/l)\Delta^1 m_2 + (\hat{x}_1/l)\Delta^2 m_2 \\ \Delta M_3 &= (1 - \hat{x}_1/l)\Delta^1 m_3 + (\hat{x}_1/l)\Delta^3 m_3, \quad 0 \le \hat{x}_1 \le l \end{aligned} \tag{A2}$$

where Δn, Δm_1, and $\Delta^\alpha m_i$ $(i = 2, 3; \alpha = 1,2)$ are the element nodal quantities defined in Eq. (6). A constant field is used for ΔN and ΔM_1, and a linear interpolation is employed for the stress couple resultants ΔM_2 and ΔM_3. Corresponding to the increments of the stress and stress couple resultants, the increment of the complementary energy density, ΔW_c, takes the form

$$\Delta W_c = \frac{1}{2}\left[\frac{(\Delta N)^2}{EA} + \frac{(\Delta M_1)^2}{GJ} + \frac{(\Delta M_2)^2}{EI_2} + \frac{(\Delta M_3)^2}{EI_3}\right] \tag{A3}$$

The stress–strain relations between the conjugate pairs of the mechanical and kinematic variables are of the form

$$\begin{aligned} &\frac{\partial \Delta W_c}{\partial(\Delta N)} = \Delta h \\ &\frac{\partial \Delta W_c}{\partial(\Delta M_1)} = \Delta\kappa_1 \\ &\frac{\partial \Delta W_c}{\partial(\Delta M_2)} + \delta(\hat{x}_1)\Delta^1\phi_2 + \delta(\hat{x}_1 - l)\Delta^2\phi_2 = -\Delta\kappa_2 \\ &\frac{\partial \Delta W_c}{\partial(\Delta M_3)} + \delta(\hat{x}_1)\Delta^1\phi_3 + \delta(\hat{x}_1 - l)\Delta^2\phi_3 = \Delta\kappa_3 \end{aligned} \tag{A4}$$

in which δ is the Dirac delta function and $\delta(\hat{x}_1 - x_0)\Delta\phi$ represents the effects of the rotational springs at the element ends. As shown in Eq. (A4), the bending curvatures are discontinuous at the element ends because of the presence of the rotational springs at the ends.

The weak form of the compatibility conditions is considered here for the element as a whole instead of the pointwise conditions. If one lets $\Delta\nu$ be the test functions (or the variations) for ΔN, $\Delta\mu_i(i = 1, 2, 3)$ be the test functions (or variations) for ΔM_i, then the weak form of Eq. (A4) becomes

$$\begin{aligned} \int_0^l \frac{\partial \Delta W_c}{\partial(\Delta N)}\Delta\nu \mathrm{d}\hat{x}_1 &= \int_0^l \Delta h \Delta\nu \mathrm{d}\hat{x}_1 \\ &= \Delta\nu \int_0^l \Delta u_{1,1}^* \mathrm{d}\hat{x}_1 = \Delta\nu\Delta H \end{aligned} \tag{A5}$$

$$\begin{aligned} \int_0^l \frac{\partial \Delta W_c}{\partial(\Delta M_1)}\Delta\mu_1 \mathrm{d}\hat{x}_1 &= \int_0^l \Delta\theta_{1,1}^* \Delta\mu_1 \mathrm{d}\hat{x}_1 \\ &= (\Delta^2\theta_1^* - \Delta^1\theta_1^*)\Delta\mu_1 \end{aligned} \tag{A6}$$

$$\begin{aligned} \int_0^l \frac{\partial \Delta W_c}{\partial(\Delta M_2)}\Delta\mu_2 \mathrm{d}\hat{x}_1 &+ \Delta^1\phi_2\Delta^1\mu_2 + \Delta^2\phi_2\Delta^2\mu_2 \\ &= \Delta^2\theta_2^*\Delta^2\mu_2 - \Delta^1\theta_2^*\Delta^1\mu_2 \end{aligned} \tag{A7}$$

$$\begin{aligned} \int_0^l \frac{\partial \Delta W_c}{\partial(\Delta M_3)}\Delta\mu_3 \mathrm{d}\hat{x}_1 &+ \Delta^1\phi_3\Delta^1\mu_3 + \Delta^2\phi_3\Delta^2\mu_3 \\ &= \Delta^2\theta_3^*\Delta^2\mu_3 - \Delta^1\theta_3^*\Delta^1\mu_3 \end{aligned} \tag{A8}$$

In Eqs. (A7) and (A8), the conditions $\int_0^l \theta_2^* \mathrm{d}\hat{x}_1 = \int_0^l \theta_3^* \mathrm{d}\hat{x}_1 = 0$ are utilized.

By substituting Eqs. (A2), (A3), and (9) into Eq. (A8), and recalling $\Delta\mu_3$ is the variation of ΔM_3, one obtains

$$\{\Delta^1\mu_3, \Delta^2\mu_3\} \frac{l}{EI_3} \begin{bmatrix} 2 + a_3 & 1 \\ 1 & 2 + b_3 \end{bmatrix} \begin{Bmatrix} \Delta^1 m_3 \\ \Delta^2 m_3 \end{Bmatrix} = \{\Delta^1\mu_3, \Delta^2\mu_3\} \begin{Bmatrix} -\Delta^1\theta_3^* \\ \Delta^2\theta_3^* \end{Bmatrix} \tag{A9}$$

where a_3 and b_3 are the parameters defined in Eq. (12). After some simple mathematical manipulations, it follows from Eq. (A9) that

$$\begin{Bmatrix} \Delta^1 m_3 \\ \Delta^2 m_3 \end{Bmatrix} = \boldsymbol{T}_3 \begin{Bmatrix} -\Delta^1\theta_3^* \\ \Delta^2\theta_3^* \end{Bmatrix} \tag{A10}$$

in which $\boldsymbol{T}_3$ is the 2×2 matrix introduced in Eq. (12). Following the similar manner for Eqs. (A5), (A6), and (A7), one finally obtains Eq. (10).

Acknowledgments

This work was supported by the Air Force Office of Scientific Research. This support is gratefully acknowledged. The assistance of Brenda Bruce in preparing the manuscript is noted with appreciation.

References

[1]Jones, S. W., Kirby, P. A., and Nethercot, D. A., "Column with Semi-Rigid Joints," *Journal of Structural Division of ASCE*, Vol. 108, No. ST2, 1982, pp. 361–372.

[2]Gaul, L., "Wave Transmission and Energy Dissipation at Structural and Machine Joints," Design Engineering Technical Conference, Hartford, CT, Sept. 20–23, 1981, ASME Paper 81-DET-17.

[3]Kwan, W. D., "The Dynamic Response of One-Degree of Freedom Bilinear Hysteretic System," *Proceedings of the 3rd World Conference on Earthquake Engineering*, 1965.

[4]Asano, K., and Iwan, W. D., "An Alternative Approach to the Random Response of Bilinear Hysteretic System," *Earthquake Engineering and Structure Dynamics*, Vol. 12, 1984, pp. 229–236.

[5]Capecchi, D., and Vestloni, F., "Steady-State Analysis of Hysteretic System," *Journal of Engineering Mechanics of ASCE*, Vol. 111, No. 12, 1985, pp. 1515–1531.

[6]Hertz, T. J., and Crawley, E. F., "The Effect of Scale on the Dynamics of Flexible Space Structures," Rept. SSL 18–81, Sept. 1983.

[7]Atluri, S. N., and Amos, A. K. (eds.), *Large Space Structures: Dynamics and Control*, Springer-Verlag, New York, 1988.

[8]Ramberg, W., and Osgood, W. R., "Description of Stress-Strain Curves by Three Parameters," NASA Technical Rept. NS02, 1943.

[9]Ang, K. M., and Morri, G. A., "Analysis of Three-Dimensional Frames with Flexible Beam-Column Connections," *Canadian Journal of Civil Engineering*, Vol. 11, 1984, pp. 245–354.

[10]Shi, G., and Atluri, S. N., "Static and Dynamic Analysis of Space Frames with Nonlinear Flexible Connections," *International Journal of Numerical Methods of Engineering*, Vol. 28, 1989, pp. 2635–2650.

[11]Shi, G., and Atluri, S. N., "Elasto-Plastic Large Deformation Analysis of Space-Frames: A Plastic-Hinge and Stress-Based Explicit Derivation of Tangent Stiffnesses," *International Journal of Numerical Methods of Engineering*, Vol. 26, 1988, pp. 589–615.

[12]Beskos, D. E., and Narayanan, G. V., "Dynamic Response of Frameworks by Numerical Laplace Transform," *Computational Methods in Applied Mechanical Engineering*, Vol. 37, No. 3, 1979, pp. 289–307.

[13]Arbabi, F., "Drift of Flexible Connection Frames," *Computation and Structure*, Vol. 15, No. 2, 1982, pp. 103–108.